Time Difference Between the 1854 CE Ansei–Tokai and Ansei–Nankai Earthquakes Estimated from Distant Tsunami Waveforms on the West Coast of North America

Satoshi Kusumoto (kusumotos@jamstec.go.jp)
JAMSTEC: Kaiyo Kenkyu Kaihatsu Kiko https://orcid.org/0000-0002-6799-1772
Kentaro Imai
JAMSTEC: Kaiyo Kenkyu Kaihatsu Kiko
Takane Hori
JAMSTEC: Kaiyo Kenkyu Kaihatsu Kiko

Research Article

Keywords: Historical earthquakes, Historical tsunamis, 1854 CE Ansei–Nankai tsunami, Time difference between Ansei–Tokai and Ansei–Nankai earthquakes, Historical materials, Numerical simulation of trans-Pacific tsunami

Posted Date: September 3rd, 2021

DOI: https://doi.org/10.21203/rs.3.rs-861187/v1

Version of Record: A version of this preprint was published at Progress in Earth and Planetary Science on January 5th, 2022. See the published version at https://doi.org/10.1186/s40645-021-00458-z.

Time Difference Between the 1854 CE Ansei–Tokai and Ansei–Nankai Earthquakes Estimated from Distant Tsunami Waveforms on the West Coast of North America

Satoshi Kusumoto[1]

Corresponding author

Email: kusumotos@jamstec.go.jp

Kentaro Imai[1]

Email: imaik@jamstec.go.jp

Takane Hori[1]

Email: horit@jamstec.go.jp

[1] Research Institute for Marine Geodynamics, Research and Development Center for Earthquake and Tsunami Forecasting, Japan Agency for Marine-Earth Science and Technology, 3173–25 Showa-machi, Kanazawa, Yokohama, 236-0001, Japan

Abstract

We estimated the time difference between the 1854 CE Ansei–Tokai and Ansei–Nankai earthquakes from tidal records of two tide gauge stations (San Francisco and San Diego) on the west coast of North America. The first signals of the Ansei–Tokai tsunami were apparent, whereas those of the Ansei–Nankai tsunami were obscured by the later waves of the Ansei–Tokai tsunami. Waveforms of the Ansei–Nankai tsunami simulated with non-linear dispersive wave theory by assuming an origin time of 07:00 GMT on 24 December arrived earlier than in the observations. The normalized root mean square and the misfit between the simulated and observed waveforms of the Ansei–Nankai tsunami showed a time difference between them of approximately 0.4 h. This finding suggests that the actual origin time of the Ansei–Nankai tsunami was approximately 07:24 GMT on 24 December. A previous study estimated the origin time of the Ansei–Tokai tsunami to be about 00:30 GMT on 23 December. Thus, we concluded that the time difference between the 1854 CE Ansei–Tokai and Ansei–Nankai tsunamis was 30.9 h. Despite the significant difference in the time resolution between the seasonal timekeeping system used in Japan in 1854 and waveform digitization, our result is roughly in agreement with historical descriptions of the tsunamis, suggesting that such information can be effectively used to determine the origin times of historical earthquakes.

Keywords

Historical earthquakes, Historical tsunamis, 1854 CE Ansei–Nankai tsunami, Time difference between Ansei–Tokai and Ansei–Nankai earthquakes, Historical materials, Numerical simulation of trans-Pacific tsunami

1. Introduction

The Nankai Trough subduction zone has repeatedly generated large earthquakes accompanied by tsunamis (e.g., Ando, 1975; Ishibashi, 2004). The fault region has been divided into six segments (e.g., Garrett et al., 2016; Fujiwara et al., 2020), and two main rupture patterns are observed: in the first, all segments rupture simultaneously, whereas in the second, different segments rupture at different times, with a time lag between ruptures of a few hours to years. The 1707 CE Hoei Nankai earthquake is an example of the first pattern, whereas the 1854 CE Ansei–Tokai and Ansei–Nankai earthquakes and the 1944 CE Showa–Tonankai and 1946 CE Showa–Nankai earthquakes are examples of the second pattern. The 1944 CE and 1946 CE events occurred about two years apart (e.g., Imai et al., 2006), and the two 1854 events approximately 30–32 h apart (e.g., Usami, 2003; Central Disaster Management Council, 2005; Matsu'ura, 2017). Thus, Nankai Trough megathrust earthquakes exhibit diverse behaviors.

The estimated moment magnitude of the 1854 Ansei–Tokai earthquake was Mw 8.4–8.6, and that of the Ansei–Nankai earthquake was Mw 8.5–8.7 (e.g., Cabinet Office Committee for

Modeling a Nankai Trough Megaquake, 2015; Building Research Institute, 2019). Furthermore, both of these earthquakes generated huge tsunamis. In this study, we focused on the time difference between the 1854 CE Ansei–Tokai and Ansei–Nankai earthquakes. In 1854, a seasonal time system was used in Japan; the day and night were separately divided into equal parts and the length of each time unit changed seasonally along with the changing sunrise and sunset times. As a result, reported origin times for these earthquakes may be not accurate. In contrast, the signals of the tsunamis generated by these earthquakes were recorded by tide stations on the west coast of North America using the fixed time system in which each day is divided into 24 h of equal length (e.g., Bache, 1856; Satake, 2020). Although there are several problems with the observed tsunami waveforms (e.g., the hydraulic filter at the time of observation is unknown), by comparing them with calculated waveforms, they can be used to quantitatively evaluate the tsunami origin time and time difference. In fact, Kusumoto et al. (2020) estimated the origin time of the 1854 CE Ansei–Tokai tsunami to be 00:30 on 23 December by comparing the tsunami waveforms observed at stations on the west coast of North America with calculated waveforms. In this study, we first estimated the origin time of the 1854 CE Ansei–Nankai tsunami by comparing observed and simulated waveforms. Then, we calculated the time difference between the 1854 CE Ansei–Tokai and Ansei–Nankai earthquakes by using our estimated origin time for the Ansei–Nankai tsunami and the origin estimated by Kusumoto et al. (2020) for the Ansei–Tokai tsunami and compared the result with historical descriptions of the two earthquakes and tsunamis.

2. Observations of the 1854 CE Ansei–Tokai and Ansei–Nankai Earthquakes

2.1 Historical materials

The 1854 CE Ansei–Tokai and Ansei–Nankai earthquakes and tsunamis are summarized in Historical Documents on Earthquakes in Japan, New Collection. This is a catalog containing historical documents with many descriptions of these events. All materials for the Ansei–Tokai and Ansei–Nankai earthquakes use the seasonal timekeeping system in use at the time, and it is very difficult to convert descriptions from different prefectures using that timekeeping system to the local time system because sunrise and sunset times differed depending on location. Therefore, we focused on historical materials from Wakayama Prefecture, which is the regional boundary between the Ansei–Tokai and Ansei–Nankai earthquake epicenters (Earthquake Research Institute of the University of Tokyo, 1987, 1989, 1994; Usami, 2008, 2012). At the time of the earthquake, sunrise and sunset in Wakayama Prefecture occurred at 07:03 and 16:56 local time, respectively (National Astronomical Observatory of Japan, 1994). Using these times, we converted the time descriptions in the historical materials to local time. Here, we focus on three reliable contemporary sources from Wakayama Prefecture.

"Kotoki", a report written in Japanese by Mr. Iwateya Heibei, a Japanese lacquerware worker who lived in Fukagawa–Kuroe city in the western part of the prefecture, is one of the most reliable contemporary documents for the Ansei–Tokai and Ansei–Nankai earthquakes (Yanagikawa, 1977). According to this report, strong shaking occurred at 08:20 local time on 23 December and again at 16:30 local time the next day. He did not report the Ansei–Tokai tsunami, but the Ansei–Nankai

96 tsunami caused serious damage on 24 December. This tsunami arrived about 50 min after the
97 earthquake and repeated waves struck Fukagawa–Kuroe city, with the third wave being the largest.
98 On the basis of this description, the time difference between the Ansei–Tokai and Ansei–Nankai
99 earthquakes can be estimated as approximately 32 h.

100 Another contemporary description is “Knowledge for Large Earthquake and Tsunami”, an
101 inscription on a monument erected in 1856 CE by Saint Zencho (Syoku), a priest of the Jinsen Temple
102 who lived in Yuasa city in the western part of the prefecture (e.g., Hatori, 1980; Ishibashi et al., 2017).
103 According to this monument, large earthquakes occurred at 10:10 local time on 23 December and at
104 15:40 local time on 24 December. A sudden rise and fall of the tide occurred on 23 December that
105 caused no damage, but on 24 December, a large tsunami destroyed houses, ships, and warehouses and
106 caused catastrophic damage to the entire settlement. On the basis of this description, the time
107 difference between the Ansei–Tokai and Ansei–Nankai earthquakes can be inferred to be about 30 h.

108 The “Diary of Koza Kirimeya”, written in Japanese by the Kirimeya owner, who lived in
109 Koza city in the southern part of the prefecture, is also a reliable contemporary document for the
110 Ansei–Tokai and Ansei–Nankai earthquakes (e.g., Hamahata, 1977; Imai et al., 2017). According to
111 this diary, strong shaking occurred at 10:10 LT on 23 December and 15:40 local time on 24 December.
112 The Ansei–Tokai tsunami arrived immediately, but was not high. The Ansei–Nankai tsunami
113 repeatedly struck, and the second wave was the highest. On the basis of this account, the time
114 difference between the Ansei–Tokai and Ansei–Nankai earthquakes can again be estimated to be

115 approximately 30 h.

116

117 **2.2 Instrumental observations**

118 In 1853, tide gauge stations were installed at three sites on the west coast of the United States:
119 Astoria, Oregon, and San Francisco and San Diego, California (U.S. Coastal Survey, 1855, Fig. 1).
120 These stations used a mechanical clock to record accurate times of high and low tides. Between 23
121 and 25 December 1854 CE, rapid rises and falls of seawater were observed at these tide gauge stations.
122 Two years later, these abnormal seawater rises and falls were recognized as the 1854 CE Ansei–Tokai
123 and Ansei–Nankai tsunamis, after they had traversed the Pacific Ocean (e.g., Bache, 1856; Omori,
124 1913).

125 In this study, we used only the tsunami signals recorded at the tide gauge stations in San Francisco
126 and San Diego because the tsunami signal observed at the Astoria tide gauge station was considered
127 too ambiguous to use. The high noise level was possibly caused by storm surges or the tsunami; a
128 sketch of the Pacific Northwest coast about 55 km north of Astoria published in 1857 shows flooding
129 that occurred between 23 and 25 December (Cooper, 1853–1854; Tolkova et al., 2015).

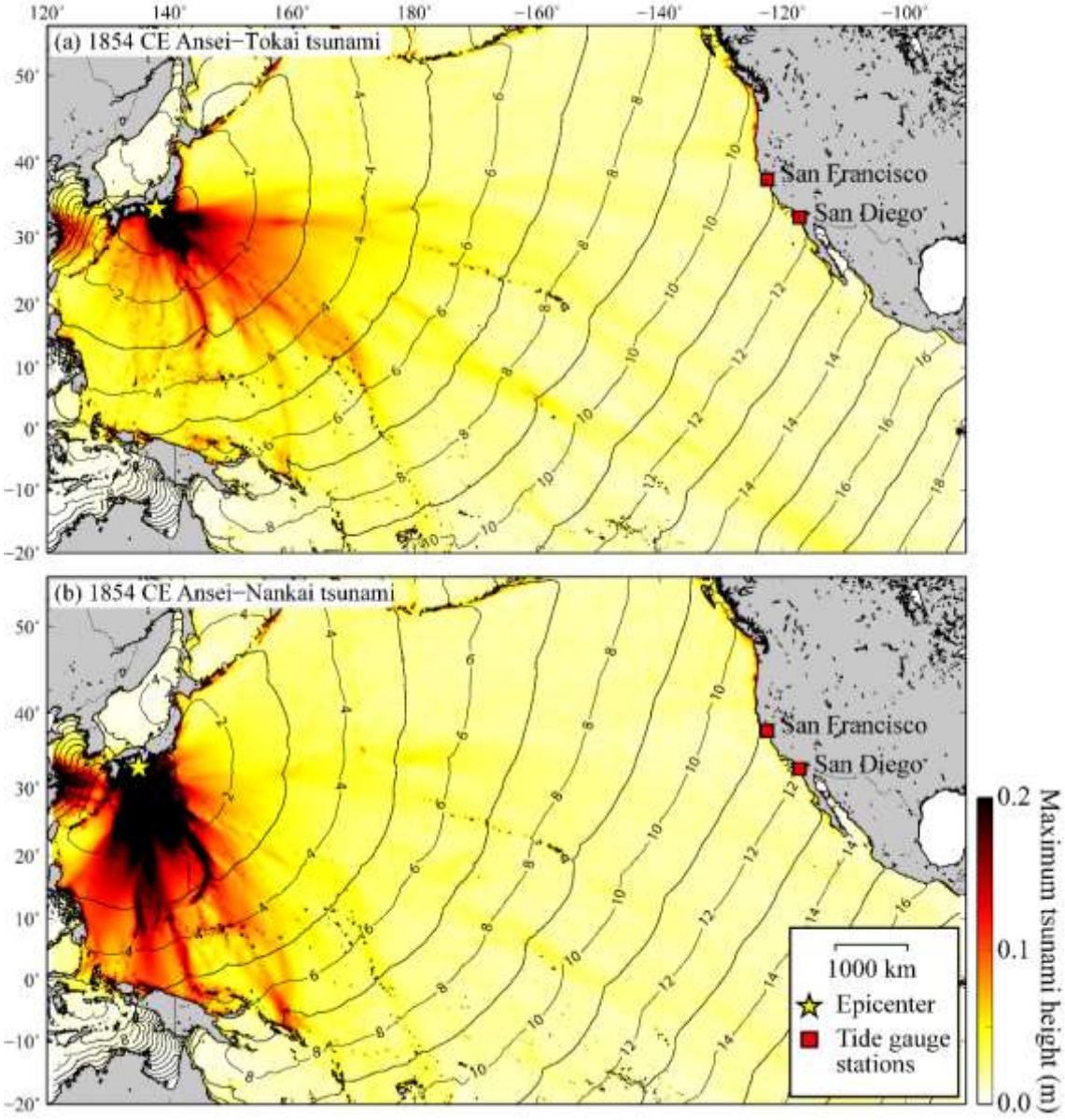

130

131 **Fig. 1** Distributions of maximum tsunami heights and tsunami travel times of the 1854 CE (**a**) Ansei–

132 Tokai and (**b**) Ansei–Nankai earthquakes. The contour interval is 1 h. The earthquake epicenters are

133 shown by yellow stars, and the locations of the North American tide gauge stations are shown by red

134 squares.

135

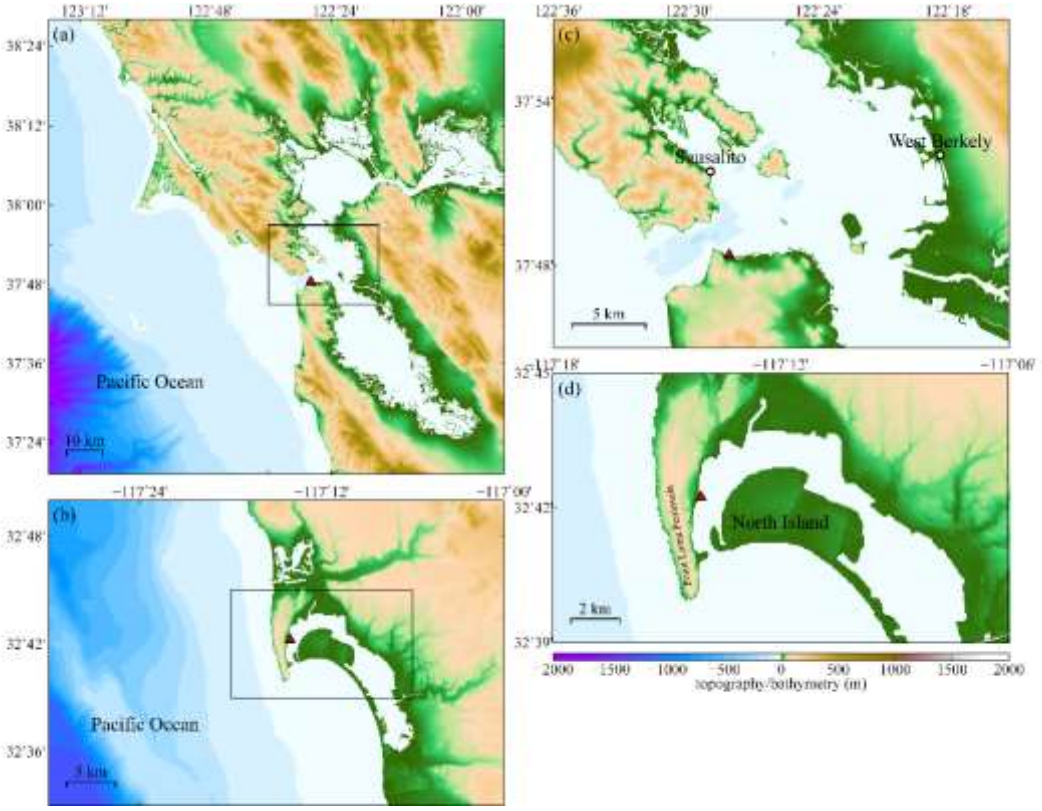

136

137 **Fig. 2** Topography and bathymetry around the (**a, c**) San Francisco and (**b, d**) San Diego tide gauge

138 stations. These data were manually reproduced based on old maps, and coastal structures were

139 manually removed by referring to old maps. Red triangles show the locations of the tide gauge stations

140 in 1854 CE.

141

142 **3. Numerical analysis**

143 Numerical simulation of trans-Pacific tsunami propagation was performed by using the staggered

144 leap-frog scheme in the JAGURS tsunami simulation code (e.g., Baba et al., 2017). Trans-Pacific

145 tsunami propagation was calculated on the basis of two-dimensional non-linear dispersive wave theory

146 with Coriolis force and Boussinesq terms in a spheroidal coordinate system. The governing equations

147 are expressed as follows:

148 $$\frac{\partial M}{\partial t}+\frac{1}{R\sin\theta}\frac{\partial}{\partial\varphi}\left(\frac{M^2}{H+\eta}\right)+\frac{1}{R}\frac{\partial}{\partial\theta}\left(\frac{MN}{H+\eta}\right)$$

149 $$=-\frac{g(H+\eta)}{R\sin\theta}\frac{\partial h}{\partial\varphi}-fN-\frac{gn^2}{(H+\eta)^{7/3}}M\sqrt{M^2+N^2}$$

150 $$+\frac{H^2}{3R\sin\theta}\frac{\partial}{\partial\varphi}\left[\frac{1}{R\sin\theta}\left(\frac{\partial^2 M}{\partial\varphi\partial t}+\frac{\partial^2(N\sin\theta)}{\partial\theta\partial t}\right)\right] \quad (1)$$

151 $$\frac{\partial N}{\partial t}+\frac{1}{R\sin\theta}\frac{\partial}{\partial\varphi}\left(\frac{MN}{H+\eta}\right)+\frac{1}{R}\frac{\partial}{\partial\theta}\left(\frac{N^2}{H+\eta}\right)$$

152 $$=-\frac{g(H+\eta)}{R}\frac{\partial h}{\partial\theta}+fM-\frac{gn^2}{(H+\eta)^{7/3}}N\sqrt{M^2+N^2}$$

153 $$+\frac{H^2}{3R}\frac{\partial}{\partial\theta}\left[\frac{1}{R\sin\theta}\left(\frac{\partial^2 M}{\partial\varphi\partial t}+\frac{\partial^2(N\sin\theta)}{\partial\theta\partial t}\right)\right] \quad (2)$$

154 where M and N are the discharge fluxes in the longitudinal (φ) and co-latitudinal (θ) directions,
155 respectively, H is the water depth of the ocean, η is the wave height, g is gravity, t is time, R is
156 the radius of the Earth, f is the Coriolis parameter, and n is Manning's roughness coefficient. The
157 volume change per unit time must be equal to the flow rate of water into the volume. Therefore, the
158 continuity equation is:

159 $$\frac{\partial\eta}{\partial t}=-\frac{1}{R\sin\theta}\left[\frac{\partial M}{\partial\varphi}+\frac{\partial(N\sin\theta)}{\partial\theta}\right] \quad (3)$$

160 Trans-Pacific tsunamis exhibit a phase delay owing to the elasticity of the Earth and the vertical
161 compressibility of seawater (e.g., Allgeyer and Cummins, 2014; Watada et al., 2014). Therefore, we
162 applied the Green's function that describes the response to a unit mass load concentrated at a point on
163 the surface as proposed by Allgeyer and Cummins (2014), which can be expressed as:

164 $$G\left(\boldsymbol{r}',\boldsymbol{r}\right)=\frac{R}{M_e}\sum_{n=0}^{\infty}h_n' P_n(\cos\alpha) \quad (4)$$

where $\boldsymbol{r}$ denotes a position on the Earth's surface with the point mass located at $\boldsymbol{r}'$, P_n refers to the nth Legendre polynomial, α is the angular distance between $\boldsymbol{r}'$ and $\boldsymbol{r}$, M_e is the mass of the Earth, and h_n' is the loading Love number of angular order n.

The tide gauge records reported in Omori (1913) have been digitized at 1 min intervals (Kusumoto et al., 2020). The effects on the observed tsunami waveform of filtering due to the structure of the water pipe at the tide gauge station at the time of the earthquake and changes in the hydraulic response are unknown, and there is no information available that allows them to be estimated. Therefore, we extracted the high-energy period band from the amplitude spectrum of the observed waveforms as follows. First, the amplitudes were normalized by the maximum amplitude in the time window covered by the simulation. Next, the bandpass filter cut-off period was determined from the amplitude spectrum of the observed waveforms. The tidal components were removed by applying a high-pass filter with a cut-off period of 128 min. Figure 4 shows the resulting amplitude spectrum. The maximum energy was observed at periods of 30–80 min, and when the period was 16 min, the energy level was approximately 1/10 of the maximum. Therefore, the cut-off period of the low-pass filter was set to 16 min. The time resolution was set to 0.1 h, which is 1/10 of the time unit of the original recording.

As the tsunami source model for the 1854 CE Ansei–Tokai and Ansei–Nankai earthquakes, we used the An'naka model, which was inferred from tsunami inundation and run-up heights (Table 1; An'naka et al., 2003). Crustal deformation, including horizontal displacement on the seafloor slope,

was computed for the source model (e.g., Okada, 1985; Tanioka and Satake, 1996), and the Kajiura filter was applied to convert crustal displacement to initial sea-surface displacement (Kajiura, 1963). To numerically model the tsunami, we adopted a nested grid system in which the nested grids included 162, 54, 18, 6, and 2 arc-seconds in the spherical coordinate system. To produce the nested grid system, the General Bathymetric Chart of the Oceans (https://www.gebco.net/data_and_products/gridded_bathymetry_data/gebco_2021/) and high-resolution (1/3 arc-second) coastal digital elevation and depth models from the U.S. National Oceanic and Atmospheric Administration were combined and resampled. Coastal structures constructed after 1854 CE were manually removed by referring to old topographic maps. A time step of 0.5 s was used in our simulations to ensure computational stability of the finite-difference algorithm with the finest grid.

The first signal of the Ansei–Nankai tsunami was obscured by later waves of the Ansei–Tokai tsunami. Therefore, we conducted a wavelet analysis of the observed waveforms to judge the arrival time of the Ansei–Nankai tsunami by applying Wavelet Analysis Package Software developed by Torrence and Compo (1998). We used the Morlet function with a scaling parameter as the wavelet mother function.

To compare the simulated and observed waveforms, we used the normalized root mean square (NRMS) and the NRMS misfit values calculated as follows:

$$\mathrm{NRMS}_k = \frac{\sqrt{\sum_{i=1}^{N}(\mathrm{obs}_i - \mathrm{sim}_i)^2}}{\sqrt{\sum_{i=1}^{N}\left(\mathrm{obs}_i - \overline{\mathrm{obs}}\right)^2}} \qquad (5)$$

$$\mathrm{NRMS\ \ misfit} = \frac{\sum_{k=1}^{M}\mathrm{NRMS}_k}{M} \qquad (6)$$

where NRMS_k is the NRMS for San Francisco or San Diego, N is the number of sampled records at the station, obs_i and sim_i are observed and simulated waveforms, respectively, and $\overline{\mathrm{obs}}$ is the average of the observed waveform at each station. M is the number of stations; thus, $M = 2$ (i.e. San Francisco and San Diego). The simulations are consistent with the observations if the indicator values are close to zero.

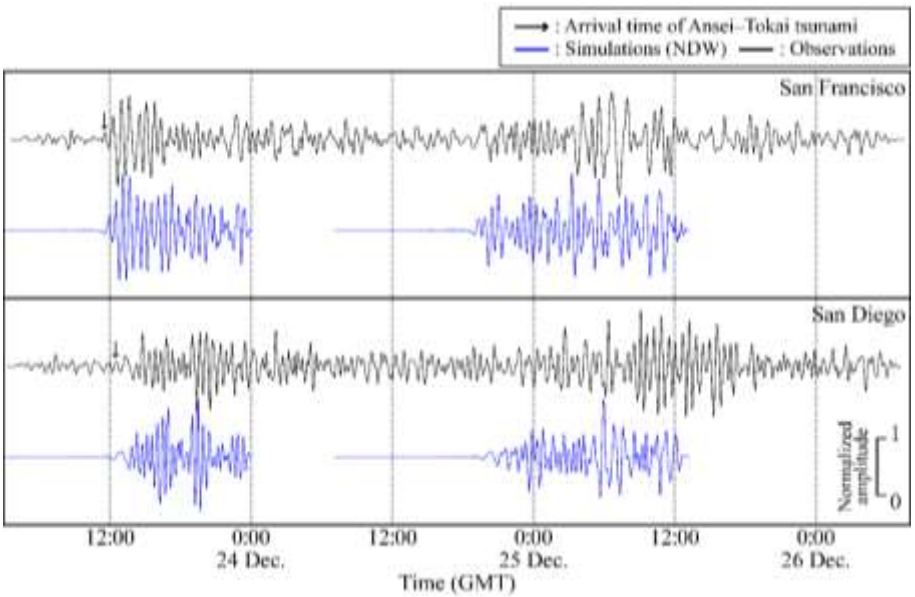

Fig. 3 Comparison of observations and non-linear dispersive wave (NDW) simulation results for the San Francisco and San Diego tide gauge stations. Black and blue curves show the observed and simulated waveforms, respectively, after application of low and high bandpass filters with cut-off

periods of 16 and 128 min, respectively.

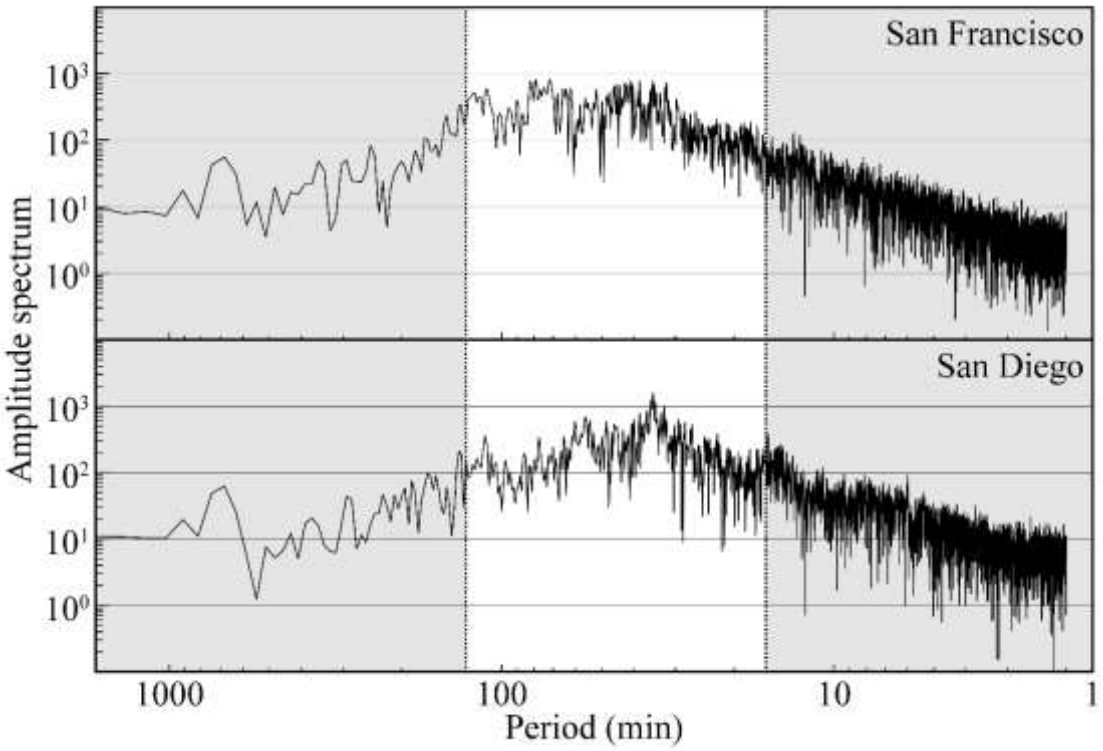

Fig. 4 Amplitude spectrums of the observed waveforms at the San Francisco and San Diego tide gauge stations. Portions of the energy band removed by application of the low and high bandpass filters (cut-off periods of 16 and 128 min, respectively) are shaded gray.

Table 1 Fault parameters of the 1854 CE Ansei–Tokai and Ansei–Nankai earthquakes

Subfault No.	Length (km)	Width (km)	Depth (km)	Strike (deg)	Dip (deg)	Rake (deg)	Slip (m)	Latitude (deg N)	Longitude (deg E)
N1	120	50	6.4	193	20	71	5.27	35.120	138.706
N2	205	100	4.1	246	10	113	5.50	33.823	138.235
N3	155	100	7.8	251	12	113	4.80	33.006	136.074
N4	125	120	10.1	250	8	113	8.70	32.614	134.481

4. Results and discussion

4.1 Characteristics of the tsunami signals

The observed and simulated waveforms at the San Francisco and San Diego tide gauge stations are compared in Fig. 3. The first signals of the 1854 CE Ansei–Tokai tsunami were apparent, whereas those of the 1854 CE Ansei–Nankai earthquake were obscured by later waves of the Ansei–Tokai tsunami. Comparing the initial observed waveforms of the Ansei–Tokai and Ansei–Nankai tsunamis at each tide station, the wavelength of the Ansei–Nankai tsunami was relatively longer than that of the Ansei–Tokai tsunami. This characteristic was reproduced by the numerical simulation. Near San Francisco and San Diego, the longer wavelength of the Ansei–Nankai tsunami, which was generated in the direction parallel to the trench axis, relative to that of the Ansei–Tokai tsunami, which was generated in the direction orthogonal to the trench axis, probably reflects the relationship between the direction of the fault strike and the orientation of the west coast of North America.

In the wavelet analysis results for the observed waveforms (Fig. 5), the Ansei–Tokai tsunami was characterized by dispersive waves that subsequently became protracted, whereas the Ansei–Nankai tsunami was characterized initially by small wave packets and subsequently by large-amplitude, high-energy waves. At the San Francisco tide gauge station, the periods of the later waves were dominantly 25–100 min for the Ansei–Tokai tsunami and 25–133 min for the Ansei–Nankai tsunami. The dominant period of the Ansei–Nankai tsunami waves roughly matches the fundamental oscillation (period about 116 min) between the Sausalito and West Berkeley sides of San Francisco Bay for waves incident on the Golden Gate (Honda et al., 1908). Therefore, the later waves of the Ansei–Nankai tsunami may correspond to the oscillations in San Francisco Bay. In contrast, at the San Diego tide gauge station, the dominant period had an upper limit of about 70 min.

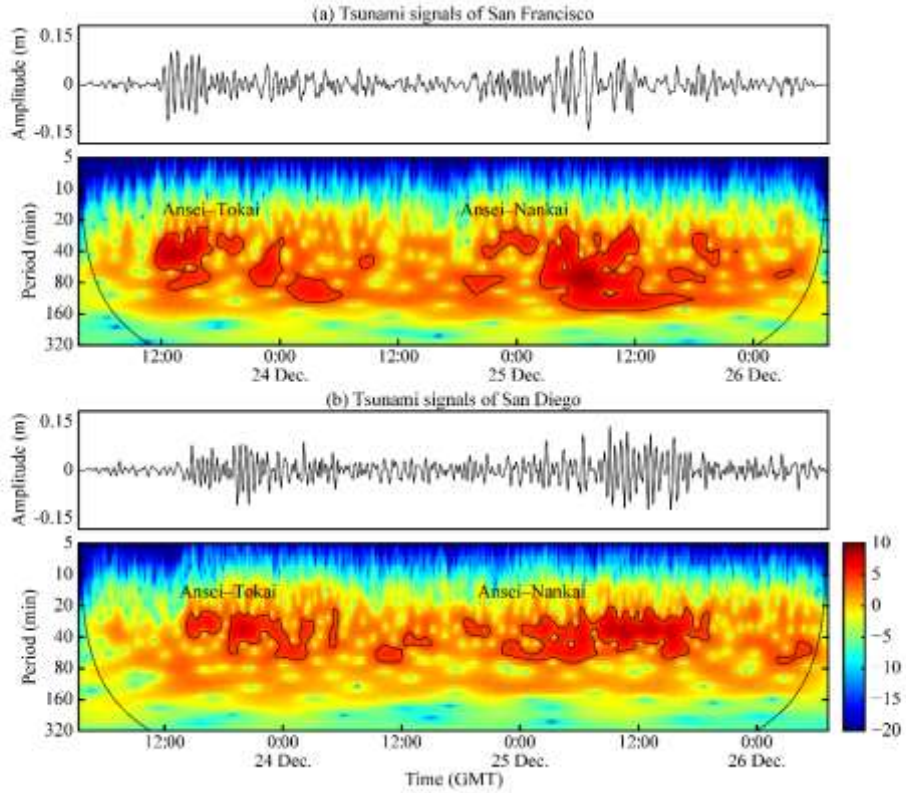

Fig. 5 Wavelet analysis results for the tsunami signals recorded at the (**a**) San Francisco and (**b**) San Diego tide gauge stations. The amplitudes have not been normalized. Contour lines show the 95% confidence interval.

4.2 Origin times of the 1854 CE Ansei–Nankai tsunamis

The simulated tsunami waves reached the west coast of North America about 11–12 h after the earthquake (Fig. 1). When the observed waveforms were compared with those simulated by assuming that the 1854 CE Ansei–Nankai tsunami originated at 07:00 GMT on 24 December, the observed waveforms lagged behind the simulated waveforms by several tens of minutes (Fig. 7). Figure 6 shows the NRMS and the NRMS misfit between the simulated waveforms and those observed at the San Francisco and San Diego tide gauge stations. The minimum NRMS misfit value was calculated when the simulated waveforms were shifted by 0.4 h. Because the simulated waveforms after shifting roughly matched the observed waveforms (Fig. 7), we estimated the origin time of the 1854 Ansei–Nankai tsunami to be 07:24 GMT on 24 December.

4.3 Time difference between the Ansei–Tokai and Ansei–Nankai earthquakes

Kusumoto et al. (2020) compared simulated and observed waveforms recorded at San Francisco and San Diego tide gauge stations and concluded that the origin time of the 1854 CE Ansei–Tokai tsunami was 00:30 GMT on 23 December. Similarly, we estimated the origin time of the 1854

Ansei–Nankai tsunami to be 07:24 GMT on 24 December. Thus, we can estimate the time difference between these earthquakes to be approximately 30.9 h.

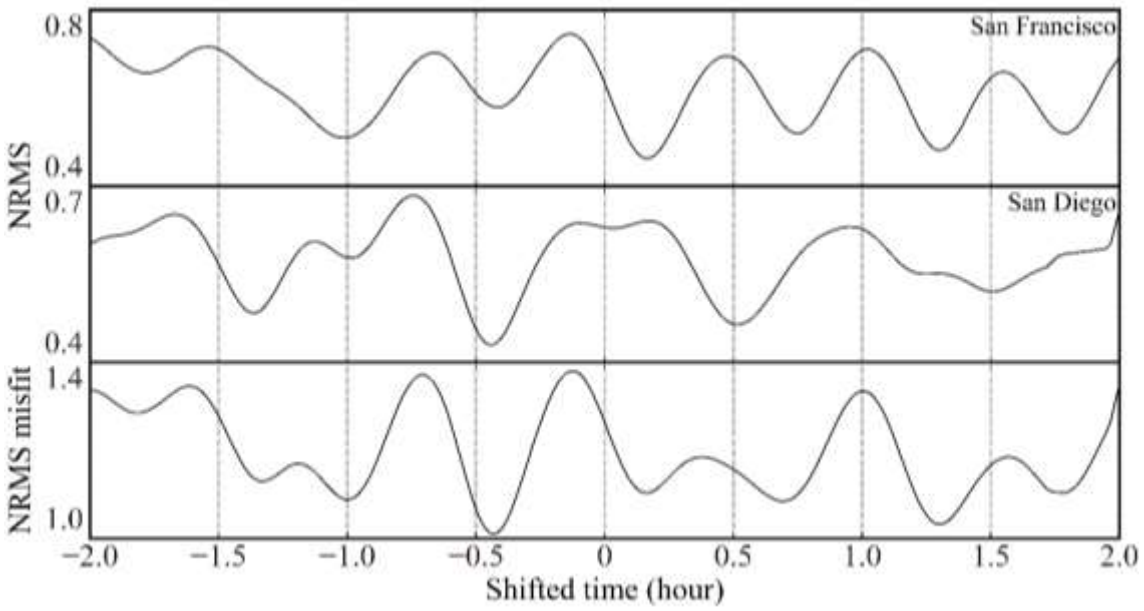

Fig. 6 Normalized root mean square (NRMS) and NRMS misfit between observed and simulated waveforms of the 1854 CE Ansei–Nankai tsunami at the San Francisco and San Diego tide gauge stations.

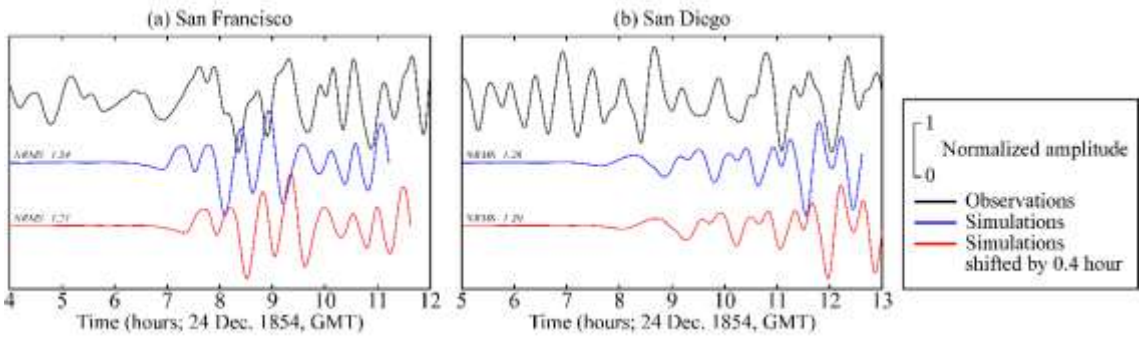

Fig. 7 Comparison of observed and simulated waveforms of the 1854 CE Ansei–Nankai tsunami

recorded at the (a) San Francisco and (b) San Diego tide gauge stations. Black, blue, and red curves show the observations, simulations, and simulations shifted by 0.4 h, respectively.

4.4 Comparison with descriptions in historical documents

According to historical descriptions in Wakayama Prefecture documents, the 1854 CE Ansei–Nankai earthquake occurred at about 16:00 local time on 24 December. Local time in Wakayama Prefecture was 9 h and 1–3 min ahead of GMT. Thus, our estimated origin time of the Ansei–Nankai tsunami of 07:24 GMT is equivalent to about 16:24 local time in Wakayama Prefecture. This result is roughly consistent with the information in the historical materials.

The time difference between the 1854 CE Ansei–Tokai and Ansei–Nankai earthquakes estimated from historical materials ranges from 30 to 32 h (e.g., Usami, 2003; Central Disaster Management Council, 2005; Matsu'ura, 2017). Thus, the resolution of the seasonal timekeeping system used in Japan at the time of the earthquakes was approximately 2 h. In contrast, the time resolution of our study was much higher at 0.1 h. Therefore, our result (30.9 h) is consistent with the time difference of about 30–32 h based on historical materials. This finding suggests that information in historical documents can be effectively used to determine the origin times of historical earthquakes if the temporal error due to the use of the seasonal timekeeping system can be tolerated.

5. Conclusions

We estimated the origin time of the 1854 CE Ansei–Nankai tsunami and the time difference between the Ansei–Tokai and Ansei–Nankai earthquakes from tidal records of the San Francisco and San Diego tide gauge stations in North America. By comparing the observations with simulations in which it was assumed that the 1854 CE Ansei–Nankai tsunami originated at 07:00 GMT on 24 December, we found that the observed waveforms of the Ansei–Nankai tsunami lagged behind the simulated waveforms by 0.4 h. Therefore, we estimated the origin time of Ansei–Nankai tsunami as 07:24 GMT on 24 December. Kusumoto et al. (2020) estimated the origin time of the 1854 Ansei–Tokai tsunami to be 00:30 GMT on 23 December; thus we estimated the time difference between the Ansei–Tokai and Ansei–Nankai tsunamis to be approximately 30.9 h. Our result is in rough agreement with descriptions in historical materials (30–32 h; e.g., Usami, 2003; Central Disaster Management Council, 2005; Matsu'ura, 2017) if the substantial difference in temporal resolution between the seasonal timekeeping system (approximately 2 hours) and the waveform digitization (0.1 h) is taken into account. This finding suggests that information in historical documents can be extremely useful for determining the origin times of historical earthquakes.

Abbreviations

NDW, non-linear dispersive wave; NRMS, normalized root mean square; GMT, Greenwich Mean Time

Declarations

Availability of data and materials

The datasets supporting the conclusions of this article are available in the supplementary information of Kusumoto et al. (2020) (available at https://doi.org/10.1785/0220200068).

Competing interests

The authors declare that they have no competing interests.

Funding

This work was supported by the Research Project for Disaster Prevention on the great Earthquakes along the Nankai trough

Authors' contributions

KI and TH contributed to the interpretation of the data. All authors read and approved the final manuscript.

Acknowledgement

We thank Professor Brian Atwater for providing information about the Astoria tide gauge station.

333

334 References

335 Allgeyer S, Cummins P (2014) Numerical tsunami simulation including elastic loading
336 and seawater density stratification, Geophys. Res. Lett., 41, pp. 2368–2375,
337 doi:10.1002/2014GL059348.

338 Ando M (1975) Source mechanisms and tectonic significance of historical earthquakes
339 along the Nankai Trough, Japan, Tectonophysics, **27**, 119–140,
340 https://doi.org/10.1016/0040-1951(75)90102-X

341 An'naka T, Inagaki K, Tanaka H, Yanagisawa K, (2003) Characteristics of great
342 earthquakes along the Nankai trough based on numerical tsunami simulation, J.
343 Earthquake Eng., 27, article 307.

344 Baba T, Allgeyer S, Hossen J, Cummins PR, Tsushima H, Imai K, Ymashita K, Kato T,
345 (2017) Accurate numerical simulation of the far–field tsunami caused by the 2011
346 Tohoku earthquake, including the effects of Boussinesq dispersion, seawater density
347 stratification, elastic loading, and gravitational potential change, Ocean Model., 111,
348 46–54, http://dx.doi.org/10.1016/j.ocemod.2017.01.002

349 Bache AD (1856) Notice of earthquake waves on the western coast of the United States,
350 on the 23rd and 25th of December, 1854, American J. Sci. Arts, 21, pp. 37–43.

351 Building Research Institute (2019) Source model and deep underground structure model

352 for long-period ground motion evaluation, Attachment 2 Appendix 3 (in Japanese)
353 https://www.kenken.go.jp/japanese/contents/topics/lpe/
354 Cabinet Office Committee for Modeling a Nankai Trough Megaquake (2015) Long-
355 period ground motion due to a huge earthquake along the Nankai Trough (in Japanese)
356 http://www.bousai.go.jp/jishin/nankai/nankaitrough_report.html
357 Central Disaster Management Council (2005) Business Continuity Guideline, Cabinet
358 Office, Government of Japan, 19–103 (in Japanese).
359 http://www.bousai.go.jp/kyoiku/kyokun/kyoukunnokeishou/rep/1854_ansei_toukai_
360 nankai_jishin/index.html
361 Cooper JG (1853-1854) NOTE BOOK, Transcribed and Reviewed by Digital Volunteers
362 Extracted April-08-2020.
363 Earthquake Research Institute (1987) New collection of historical materials on
364 earthquakes in Japan, vol S5-5-1&2. ERI, Tokyo, pp 2528 (in Japanese)
365 Earthquake Research Institute (1989) New collection of historical materials on
366 earthquakes in Japan, Suppl S. ERI, Tokyo, pp 992 (in Japanese)
367 Earthquake Research Institute (1994) New collection of historical materials on
368 earthquakes in Japan, Add. Suppl. S. ERI, Tokyo, pp 1228 (in Japanese)
369 Fujiwara O, Goto K, Ando R, Garrett E, (2020) Paleotsunami research along the Nankai
370 Trough and Ryukyu Trench subduction zones -current achievements and future

challenges. Earth-Sci. Rev. 210, 103333. https://doi.org/10.1016

Garrett E, Fujiwara O, Garrett P, Heyvaert VMA, Shishikura M, Yokoyama Y, Hubert–Ferrari A, Brückner H, Nakamura A, Batist MD (2016) A systematic review of geological evidence for Holocene earthquakes and tsunamis along the Nankai–Suruga Trough, Japan., Earth Sci. Rev., **159**, 337–357. http://dx.doi.org/10.1016/j.earscirev.2016.06.011.

Hamahata E (1977) Continued historical materials of the Kumano city, pp. 203–208

Hatori T (1980) Field Investigation of the Nankaido Tsunamis in 1707 and 1854 along the Osaka and Wakayama Coasts, West Kii Peninsula, Bull. Earthq. Res. Inst., 55 (2), pp.505–535 (in Japanese) https://repository.dl.itc.u-tokyo.ac.jp/records/33078#.YNVgI-j7RnI

Honda K, Terada T, Yoshida Y, Isitani D (1908) An investigation on the secondary undulations of oceanic tides, J. College Sci.,Imper. Univ. Tokyo, 108 pp.

Imai S, Kanamori Y, Shuto N (2006) Tsunami Digital Library, J. Gonzalo at al. (Eds.) ECDL2006, LNCS 4172, pp. 555-558. http://tsunami-dl.jp/old-content/TSUNAMI/TDL_top_e.html

Imai K, Ishibashi M, Namegaya Y, Ebina Y (2017) Field survey for tsunami trace height during the 1854 Ansei Nankai tsunami along the Wakayama Coast, Research Report of Tsunami Engineering, 33, pp. 121–130 (in Japanese).

390 Ishibashi K (2004) Status of historical seismology in Japan, Ann. Geophys., **47**(2–3), pp.
391 339–368, https://doi.org/10.4401/ag-3305
392 Ishibashi M, Maeda M, Imai K, Takahashi N, Baba T, Obayashi R, Inazumi T, (2017) The
393 tsunami monument distribution along the coast of Wakayama Prefecture, *Research*
394 *Report of Tsunami Engineering*, 33, pp. 109-120.
395 Kajiura K (1963) The leading wave of a tsunami, *Bull. Earthquake Res. Inst., Univ. Tokyo*,
396 **41**, pp. 535–571.
397 Kusumoto S, Imai K, Obayashi R, Hori T, Takahashi N, Ho TC, Uno K, Tanioka Y, Satake
398 K (2020) Origin Time of the 1854 Ansei–Tokai Tsunami Estimated from Tide Gauge
399 Records on the West Coast of North America, Seismological Research Letters, 91 (5),
400 pp. 2624-2630, https://doi.org/10.1785/0220200068
401 Matsu'ura R (2017) Earthquake Forecasting and the Large–Scale Earthquake
402 Countermeasures Act, Monogr. Seismol. Soc. Jpn., 5, pp. 15–19 (in Japanese).
403 National Astronomical Observatory of Japan (1994) Koyomi Station,
404 https://eco.mtk.nao.ac.jp/cgi-bin/koyomi/koyomix_en.cgi (Accessed 30 June 2021)
405 Okada Y (1985) Surface displacement due to shear and tensile faults in a half–space, Bull.
406 Seismol. Soc. Am., 75 (4), pp. 1135–1154.
407 Omori F (1913) An account of the destructive earthquakes in Japan, Publ. Eq. Inv. Com.,
408 68B, 1–179 (in Japanese).

409 Satake K, Heidarazadeh M, Quiroz M, Cienfuegos R (2020) History and Features of
410 Trans–oceanic Tsunamis and Implications for Paleo–tsunami Studies, Earth Sci. Rev.,
411 202, 103112, https://doi.org/10.1016/j.earscirev.2020.103112
412 Tanioka Y, Satake K (1996) Tsunami generation by horizontal displacement of ocean
413 bottom, *Geophys. Res. Lett.*, **23** (8), pp. 861–864.
414 Tolkova E, Tanaka H, Roh M (2015) Tsunami Observations in Rivers from a Perspective
415 of tsunami interaction with tide and riverine flow, Pure Appl. Geophys. 172, pp. 953-
416 968.
417 Torrence C, Compo GP (1998) A practical guide to wavelet analysis, Bull. Am. Meteorol.
418 Soc., 79, pp. 61–78.
419 U. S. Coast Survey (1855) Annual Report of the Superintendent of the Coast Survey,
420 National Oceanic and Atmosphere Administration, 288 pp.
421 Usami T (2003) Materials for comprehensive list of Japanese destructive earthquakes
422 [Latest Edition] [416]-2001. Univ Tokyo Press, Tokyo, p 605 (in Japanese)
423 Usami T (2008) Addendum of historical documents on earthquakes in Japan, 4–1&2, T.
424 Tokyo, Usami, pp. 1874 (in Japanese)
425 Usami T (2012) Addendum of historical documents on earthquakes in Japan, 5-1&2, T.
426 Usami, Tokyo, pp 1526 (in Japanese)
427 Watada S, Kusumoto S, Satake K (2014) Traveltime delay and initial phase reversal of

distant tsunamis coupled with the self–gravitating elastic Earth, J. Geophys. Res. Solid Earth, **119**, doi:10.1002/2013JB010841.

Yanagikawa K (1977) The Takanami Records by Iwateya Heibei in Kuroe, Kainan-shishi, 3, pp. 33-37 (in Japanese).